Journal of Statistical Physics, Vol. 115, Nos. 3/4, May 2004 (© 2004)

Winding Clusters in Percolation on the Torus and the Möbius Strip

Gunnar Pruessner[1] **and Nicholas R. Moloney**[2]

Received October 15, 2003; accepted November 21, 2003

Using a simulation technique introduced recently, we study winding clusters in percolation on the torus and the Möbius strip for different aspect ratios. The asynchronous parallelization of the simulation makes very large system and sample sizes possible. Our high accuracy results are fully consistent with predictions from conformal field theory. The numerical results for the Möbius strip and the number distribution of winding clusters on the torus await theoretical explanation. To our knowledge, this study is the first of its kind.

KEY WORDS: 2D-percolation; Monte-Carlo; conformal field theory; Möbius strip; torus.

1. INTRODUCTION

Since the seminal article of Langlands *et al.*,[10] percolation has enjoyed a renaissance in the last decade. Cardy's result[3] for the probability of a crossing cluster on a rectangle was the first major breakthrough of conformal field theory in critical percolation. Related to this work, Pinson calculated the probability of clusters of particular winding numbers in ref. 19, using the partition sum for the torus formulated earlier by di Francesco *et al.*[5]

In 1996 Hu and Lin showed numerically[7] that the probability of more than one percolating cluster is non-vanishing, which was proven by Aizenman[1] shortly afterwards. In fact, Cardy was able to calculate the asymptotic probability of n distinct, simultaneously crossing clusters[4]

[1] Department of Mathematics, Imperial College London, 180 Queen's Gate, London SW7 2BZ, United Kingdom; e-mail: gunnar.pruessner@physics.org

[2] Condensed Matter Theory, Blackett Laboratory, Imperial College London, Prince Consort Rd, London SW7 2BW, United Kingdom; e-mail: n.moloney@imperial.ac.uk

0022-4715/04/0500-0839/0 © 2004 Plenum Publishing Corporation

exactly. One expects similar behavior for the number of distinct, simultaneously winding clusters on the torus.

In this article we present numerical results for (multiply) winding clusters on the torus and on the Möbius strip with different aspect ratios, providing strong numerical support for the claim of conformal invariance in two dimensional percolation. Apart from the numerical results for $r = 1$ by Langlands *et al.* presented in ref. 19, the only other numerical studies of this kind, to our knowledge, is one by Ziff *et al.*,[24] who measure the probability of a cross topology for very small system sizes (16×16) and different twists on a torus with aspect ratio 1, and those by Newman and Ziff,[17, 18] who measure the probability of winding clusters on a torus with aspect ratio 1 and system sizes up to 256×256 and varying occupation probability. Also, for the Möbius strip we are only aware of studies on the Ising model.[8, 11]

1.1. Critical Percolation on the Torus

We treat site and bond percolation as the two limiting cases of the more general site-bond percolation: Sites are occupied with probability $p^{(s)}$ and bonds are activated with probability $p^{(b)}$. In site percolation all bonds are active, while in bond percolation all sites are occupied. Two sites are connected if the bond between them is active and both sites are occupied. Two sites belong to the same cluster if they are connected by a path along occupied sites and active bonds. On a torus and the Möbius strip, these paths may wind around the lattice. By our convention, (a, b) counts the number of windings in the horizontal and vertical directions, respectively. Vertical and horizontal directions are fixed by the definition of aspect ratio as the vertical circumference (waist) over the horizontal circumference (ignoring the distortion), see Fig. 1.

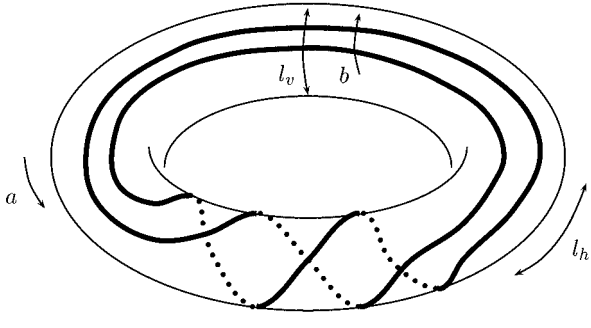

Fig. 1. A torus with $r = l_v/l_h$ and a (2, 3) winding cluster shown as a thick line. The winding directions of (a, b) are marked as such.

The topological considerations in this paper are mainly technically motivated and rather heuristic. For rigorous proofs, we refer to the standard literature.[14] On the torus, it is a topological fact that if $a = 0$ ($b = 0$) then the only path which is not homotopic to a point and does not intersect itself has $b = 1$ ($a = 1$). There is no topological difference between (a, b) and $(-a, -b)$—the direction in which these paths are taken is simply inverted. If $a \neq 0$ and $b \neq 0$ then a and b must be relative prime if the path does not intersect itself.

In the following, winding numbers (a, b) will be used in a "normalized" fashion: $a = 1$ for $b = 0$, $b = 1$ for $a = 0$, a and b are relative prime if $a \neq 0$ and $b \neq 0$, and $a \geqslant 0$. A (2, 3) path is shown in Fig. 1.

In addition to the above, we also mention the path with the so-called "cross topology."[5] Such a path is produced by intersecting a (1, 0) and a (0, 1) path.

To transfer the notion of winding from paths to clusters, one considers all (topologically different) paths within a cluster. If there is a path with non-zero winding numbers that crosses only paths which are homotopic to a point or have the same winding numbers, the cluster is assigned the winding numbers of the path. If there is no winding path at all, then this cluster itself is said to be homotopic to a point. It transpires that in any other case the cluster contains a cross-topological path and the cluster is then said to have a cross topology itself.

The *universal* probability to obtain n clusters with winding numbers (a, b) at aspect ratio r is denoted in the following by $\hat{\mathscr{P}}((a, b), n, r)$. Pinson has derived the formula[19]

$$\begin{aligned}\hat{\mathscr{P}}((a,b),\geqslant 1,r) = &\sum_{l\in\mathbb{Z}} Z_{a3l,\,b3l}(\tfrac{2}{3};r) - \tfrac{1}{2}\sum_{l\in\mathbb{Z}} Z_{a(3l+1),\,b(3l+1)}(\tfrac{2}{3};r)\\ &-\tfrac{1}{2}\sum_{l\in\mathbb{Z}} Z_{a(3l+2),\,b(3l+2)}(\tfrac{2}{3};r) - \sum_{l\in\mathbb{Z}} Z_{a2l,\,b2l}(\tfrac{2}{3};r)\\ &+\sum_{l\in\mathbb{Z}} Z_{a(2l+1),\,b(2l+1)}(\tfrac{2}{3};r) \qquad (1)\end{aligned}$$

where

$$Z_{m,n}(g;r) = \frac{\sqrt{g}}{\sqrt{r}\,\eta^2(e^{-2\pi r})}\exp\left(-\pi g\left(\frac{m^2}{r}+n^2 r\right)\right), \qquad (2)$$

and

$$\hat{\mathscr{P}}((a,b),\geqslant n,r) = \sum_{i=n}^{\infty}\hat{\mathscr{P}}((a,b),i,r). \qquad (3)$$

Here $\eta(q)$ is the Dedekind eta function

$$\eta(q) = q^{1/24} \prod_{k=1}^{\infty} (1-q^k). \tag{4}$$

Correspondingly, the probability of a cross topology is denoted by $\hat{\mathscr{P}}(\mathsf{X}, r)$, and the probability that all clusters in a given configuration are homotopic to a point is denoted by $\hat{\mathscr{P}}(0, r)$. The exact expressions for these probabilities are

$$\hat{\mathscr{P}}(\mathsf{X}, r) = \hat{\mathscr{P}}(0, r) = \tfrac{1}{2}\left(Z_c(\tfrac{8}{3}, 1; r) - Z_c(\tfrac{8}{3}, \tfrac{1}{2}; r)\right) \tag{5}$$

with

$$Z_c(g, f; r) = f \sum_{m,n \in \mathbb{Z}} Z_{fm, fn}(g; r). \tag{6}$$

In the following, we will distinguish exact results from numerical results by putting a hat on all exact quantities. Where necessary, the numerical results will also have an index indicating the system size and a superscript (s) for site percolation and (b) for bond percolation. For example, $\mathscr{P}^{(\mathrm{b})}_{N=3000^2}((1, 2), 1, 9)$ is the fraction of cases in which we observed a single $(1, 2)$ cluster in bond percolation with aspect ratio 9 and 3000^2 sites.

Multiple, distinct clusters with the *same* winding number can coexist without intersecting.[5] This, however, does not apply to a cluster with a cross topology: there can only be one such cluster on a torus. Winding clusters with incommensurable winding numbers, meanwhile, cannot coexist. Thus an entire configuration of the lattice on the torus is characterized by the winding numbers of the winding clusters, if any, and their total number.

The Möbius strip is a little more complicated in this respect. First of all, since the Möbius strip is a non-orientable surface, a reasonable definition of a spanning cluster connecting one side to the other is not possible, unlike, for example, clusters on a cylinder connecting top and bottom.[4, 20] Winding clusters behave rather surprisingly. A single winding cluster, winding around only once, is possible. Meanwhile, if two winding clusters coexist, then at least one of them must have winding number 2. In general, n winding clusters require at least $n-1$ clusters with winding number 2. In fact, all winding clusters are fully defined by the *total* number a of windings alone: If a is even, there are $a/2$ winding clusters with winding number 2. If a is odd, there are $(a-1)/2$ winding clusters with winding number 2, and 1 cluster with winding number 1. Figure 2 shows a Möbius strip with 2 winding paths adding up to a total winding number 3. The aspect ratio of

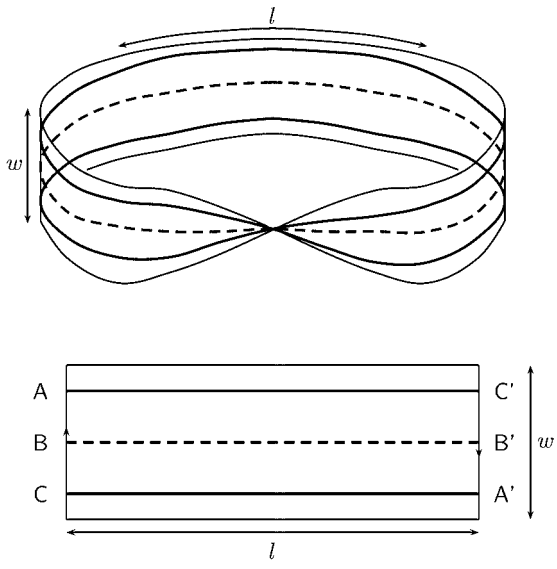

Fig. 2. A Möbius strip with two non-intersecting winding clusters: one with winding number 2 (full line, labelled A, B) and one with winding number 1 (dashed line, labelled C). On the Möbius strip, the labeled endpoints coincide with their primed counterparts. Below, the "unwrapped" lattice shows the definition of the aspect ratio, $r = w/l$.

the Möbius strip is defined as the width of the band over the path length along the band, as shown in Fig. 2.

1.2. Method

The simulation method is essentially a trivially parallelized adaptation of the Hoshen–Kopelman[6] algorithm with modified "Nakanishi label recycling."[2, 16] Master nodes assemble a large lattice from "patches" provided by slave nodes, much in the spirit of ref. 21, for example. Full details of the method may be found in ref. 15, while the detection of wrapping clusters is discussed in ref. 20. The method in principle relaxes all the standard constraints in numerical simulations of percolation, such as CPU power, memory, and network capacity, and is especially suited for calculating cluster size distributions and crossing probabilities. Here we use it to calculate probabilities of winding clusters on the torus and the Möbius strip for system sizes $N = 30000^2, 3000^2, 300^2$. Although it is known in general that finite-size effects are very small for the torus,[21] we decided nevertheless to simulate such large system sizes to investigate observables for which the strength of finite-size effects is not yet established. In fact, it transpires that $N = 300^2$ and $N = 30000^2$ do not deviate significantly.

Whether or not finite-size effects are relevant can only be known in hindsight. The random number generator is described in ref. 13, and is especially suitable for parallel applications.

2. RESULTS

In this section we first list the key parameters of the simulation. Then we discuss the assumptions and estimates of the numerical errors associated with the study. We then present the results for the torus which can be compared to Pinson's formulae (1) and (5), asymptotes for which are presented in Section 2.3. Finally, we present the results for the number distribution of multiple winding clusters and the results for the Möbius strip.

In each simulation, we have determined $\mathscr{P}_N((a,b),n,r)$ as well as $\mathscr{P}_N(0,r)$ and $\mathscr{P}_N(\mathsf{X},r)$ for site and bond percolation at the critical point, i.e., occupation probability $p^{(\mathrm{s})}=0.59274621^{(17)}$ in site percolation and activation probability $p^{(\mathrm{b})}=1/2^{(9)}$ in bond percolation.

Each simulation, parametrized by the system size N and the type of percolation (site or bond), consists of at least 10^6 realizations. The 14 different aspect ratios are: 30/30, 36/25, 45/20, 50/18, 60/15, 75/12, 90/10, 100/9, 150/6, 180/5, 225/4, 300/3, 450/2, and 900/1. While a torus with aspect ratio r is topologically identical to a torus with aspect ratio $1/r$, a Möbius strip can be joined along two different borders to form a band either of aspect ratio r or $1/r$. Thus, 27 different aspect ratios are available for the Möbius strip.

2.1. Numerical Errors

In a numerical simulation an estimate p for the probability of the occurrence of a particular property (such as 2 winding clusters with winding number (1, 3)) is measured as the average of an indicator function $f(\mathscr{C})$ of the configuration $\mathscr{C}$, which is 1, if the property is found in the configuration and 0 otherwise. As all higher moments of f are p, the variance of p is then simply estimated as $p-p^2$, so that the variance of the estimator of the probability is estimated as $(p-p^2)/(N-1)$, where N is the number of (independent) realizations.

In the following we make use of the symmetry of the torus,

$$\hat{\mathscr{P}}((a,b),n,r)=\hat{\mathscr{P}}((b,a),n,r^{-1})$$
$$\hat{\mathscr{P}}(0,n,r)=\hat{\mathscr{P}}(0,n,r^{-1})$$
$$\hat{\mathscr{P}}(\mathsf{X},n,r)=\hat{\mathscr{P}}(\mathsf{X},n,r^{-1}),$$

i.e., the results of r and $1/r$ are not independent.

2.2. Winding Clusters

One surprising result in Pinson's paper[19] is that the probability of a cluster with cross topology, $\hat{\mathscr{P}}(\mathsf{X}, r)$, is identical to the probability of no winding cluster at all, $\hat{\mathscr{P}}(0, r)$, i.e., the probability that *all* clusters are homotopic to a point. This is in perfect agreement with our numerical results.

It is obvious that there can only be one cluster with a cross topology, and that any other cluster must be homotopic to a point, i.e., if a configuration contains a cluster with a cross topology, there is no other non-trivial cluster.

Next we investigate the probability of at least one cluster with winding numbers (a, b), the exact expression for which was conjectured by Pinson to be (1). Figure 3 shows the relative deviation of the numerical results from the exact value for clusters with winding numbers (1, 0), (1, 1), and (1, 2) for $N = 30000^2$ and bond percolation. The reason why so many points seem to indicate no deviation at all is that the probability of certain types of winding clusters is extremely small. As a result, some rare types were not observed in the simulation and the resulting deviation from the exact result is approximately $\sqrt{p}/\sqrt{N-1}$, i.e., extremely small. Moreover, it should be noted that the numerical error of the evaluation of (1) increases as the probability approaches 0 or 1.

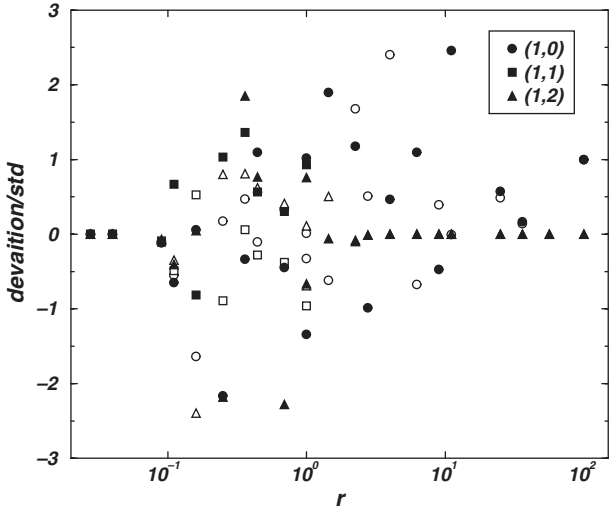

Fig. 3. The deviation of $\mathscr{P}_{N=30000^2}((a, b), \geqslant 1, r)$ from $\hat{\mathscr{P}}((a, b), \geqslant 1, r)$ (see (1)) in units of standard deviations for $(a, b) = (1, 0)$, (1, 1), (1, 2) and site (filled symbols) and bond (opaque symbols) percolation.

All our numerical findings are fully consistent with (1) for winding numbers $(1, 0)$, $(1, \pm 1)$, $(1, \pm 2)$, and $(1, \pm 3)$, in site and bond percolation. Other winding numbers occur too rarely to make any firm statements.

Percolation on a torus is mirror symmetrical, i.e.,

$$\hat{\mathscr{P}}((a, b), n, r) = \hat{\mathscr{P}}((a, -b), n, r) = \hat{\mathscr{P}}((-a, b), n, r) = \hat{\mathscr{P}}((-a, -b), n, r). \tag{7}$$

While a cluster of type (a, b) is simply identical to a cluster of type $(-a, -b)$, the windings (a, b) and $(a, -b)$ are in fact distinguishable. Since these two quantities have the same probability, their comparison affords a consistency check upon the numerics, independent of any theoretical result or finite size corrections. The numerics passed this test successfully.

2.3. Asymptotes

To discuss numerical results for the asymptotic behavior of multiple winding clusters, we must first extract an appropriate functional form to fit against from (1). A calculation closely related to the following was presented by Ziff for the problem of crossing in two-dimensional percolation[22, 23] and subsequently used in ref. 20.

It is convenient to slightly rewrite Eq. (1). Noting that all $Z_{m,n}$ enter (1) in the form $Z_{ak,bk}$, it is reasonable to define

$$\tilde{Z}((a, b); g, r) = \sqrt{\frac{g}{r}} \sum_{l \in \mathbb{Z}} \exp\left(-l^2 \pi g \left(\frac{a^2}{r} + b^2 r\right)\right), \tag{8}$$

which is just $\sqrt{g/r}\, \vartheta_3(0, \tau)$, where $\tau = ig(a^2/r + b^2 r)$ and ϑ_3 is Jacobi's theta function.[12] By using transformations of the form $\sum_l f_{2l+1} = \sum_l f_l - \sum_l f_{2l}$ one has

$$\hat{\mathscr{P}}((a, b), \geqslant 1, r) = \frac{1}{\eta(e^{-2\pi r})^2}\left(\frac{1}{2}\tilde{Z}((a, b); 6, r) - \tilde{Z}((a, b); 8/3, r) + \frac{1}{2}\tilde{Z}((a, b); 2/3, r)\right), \tag{9}$$

given appropriate convergence of the sums in (8) and (1). To find the asymptotic behaviour for $(a, b) = (1, 0)$, it is useful to rewrite Eq. (8) as

$$\tilde{Z}((a, b); g, r) = \frac{1}{\sqrt{a^2 + b^2 r^2}} \sum_{l \in \mathbb{Z}} \exp\left(-\frac{\pi}{g(a^2 + b^2 r^2)} l^2 r\right), \tag{10}$$

by applying the Poisson summation formula. From the definition of the Dedekind η-function one finds the following expansion for large r:

$$\eta^{-2}(\exp(-2\pi r)) = e^{\pi r/6}(1+2e^{-2\pi r}+5e^{-4\pi r}+10e^{-6\pi r}+\cdots). \tag{11}$$

Using (10) and (11) for the large r expansion of (9) the task boils down to ordering terms:

$$\hat{\mathscr{P}}((1,0), \geqslant 1, r) = 1-2e^{-\frac{5}{24}\pi r}+e^{-\frac{1}{2}\pi r}+2e^{-2\pi r}-4e^{-\frac{53}{24}\pi r}+3e^{-\frac{5}{2}\pi r}\cdots. \tag{12}$$

This approximation has a relative deviation from the exact result of less than 5×10^{-4} at $r=1$ and less than 10^{-8} at $r=2$.

Using $\hat{\mathscr{P}}((1,0), \geqslant 1, r) = \hat{\mathscr{P}}((0,1), \geqslant 1, 1/r)$, the corresponding expansion for small r is now based directly on (8). Thus again for large r

$$\hat{\mathscr{P}}((0,1), \geqslant 1, r) = \sqrt{\frac{2}{3r}}\,(e^{-\frac{1}{2}\pi r}-e^{-\frac{5}{2}\pi r}-e^{-\frac{9}{2}\pi r}+4e^{-\frac{35}{6}\pi r}\cdots). \tag{13}$$

At $r=1$ the relative error of this approximation is better than 3×10^{-8}, which improves to about 10^{-15} at $r=2$.

Similarly one finds for $\hat{\mathscr{P}}(\mathsf{X}, r)$

$$Z_c(f, g; r) = \frac{1}{\eta(e^{-2\pi r})^2}\,\tilde{Z}((1,0); f^2 g, r)\,\tilde{Z}((1,0); 1/(f^2 g), r) \tag{14}$$

which yields together with (11)

$$\hat{\mathscr{P}}(\mathsf{X}, r) = e^{-\frac{5}{24}\pi r}-e^{-\frac{1}{2}\pi r}-2e^{-2\pi r}+2e^{-\frac{53}{24}\pi r}-2e^{-\frac{5}{2}\pi r}\cdots \tag{15}$$

again for large r. The relative deviation is less than 9×10^{-4} at $r=1$ and about 10^{-7} at $r=2$.

2.4. Multiple Winding Clusters

Unfortunately, it is not straightforward to extend Cardy's qualitative arguments in the introduction of ref. 4 for the existence of multiple spanning clusters.

Multiple winding clusters with winding numbers other than $(1, 0)$ are very rare. In fact, we found

$$\mathscr{P}^{(s)}_{N=1000^2}((1,1), 2, 1) + \mathscr{P}^{(s)}_{N=1000^2}((1,-1), 2, 1) = 1.40(8)\times 10^{-7} \tag{16a}$$

$$\mathscr{P}^{(b)}_{N=1000^2}((1,1), 2, 1) + \mathscr{P}^{(b)}_{N=1000^2}((1,-1), 2, 1) = 1.50(10)\times 10^{-7} \tag{16b}$$

based on the data produced at the slave nodes. Probabilities for higher multiples and other winding numbers are less than about 1 in 2×10^9.

From what has been said in Section 2.3 (see also Eq. (18)) one might suspect that the probability of n distinct, simultaneously winding clusters with winding number (1, 0) behaves in the limit of small r like

$$\hat{\mathscr{P}}((1,0), n, r) \approx C((1,0), n)\, e^{-\alpha((1,0),n)/r} \sqrt{r}. \tag{17}$$

The variable $C((1, 0), n)$ denotes the amplitude for this type of winding and $\alpha((1, 0), n)$ is expected to be a second order polynomial in n.[4] Clearly, the additional factor $\sqrt{r}$ is "only" a logarithmic correction to the dominating exponential, but is in fact clearly visible in the numerics.

Nothing can be derived from Section 2.3 concerning the large r limit, since the average number of winding clusters and the variance thereof become very large.

Figure 4 shows the estimated probabilities in the form $\ln(\mathscr{P}/(1-\mathscr{P}))$.[3, 20] These probabilities have been fitted against (17) in the small r limit, the results of which are shown in Table I. Even though the choice of (17) is somewhat arbitrary for $n > 1$, very good fits are obtained. These are shown by the dashed lines in Fig. 4, which represent the fitting results of Table I fed back into (17). The main source of the numerical error is the fitting range, which is listed in the table. The range is bounded below by the smallest value of r that is supported by available data within reasonable error, and bounded above by the approximate value for r after which the asymptotic behavior terminates. The ambiguity of the fitting range is not reflected in the error bars, which indicate only the statistical error. Therefore the exact result fitted to the function (17) within the given interval should produce the values listed above.

The dotted line in Fig. 4 shows $\hat{\mathscr{P}}((1, 0), \geqslant 1, r)$, which asymptotically (small r) contains only a single winding cluster, i.e.,

$$\lim_{r \to 0} \frac{\hat{\mathscr{P}}((1,0), \geqslant 1, r) - \hat{\mathscr{P}}((1,0), 1, r)}{\hat{\mathscr{P}}((1,0), \geqslant 1, r) + \hat{\mathscr{P}}((1,0), 1, r)} = 0 \tag{18}$$

so that the amplitude $C((1, 0), 1)$ and the exponent $\alpha((1, 0), 1)$ are known exactly from (13):

$$C((1,0), 1) = \sqrt{2/3} = 0.8164909\ldots \tag{19a}$$

$$\alpha((1,0), 1) = \pi/2 = 1.5707963\ldots \tag{19b}$$

which is in very good agreement with the results in Table I, indicating that the fitting range chosen there is reasonable.

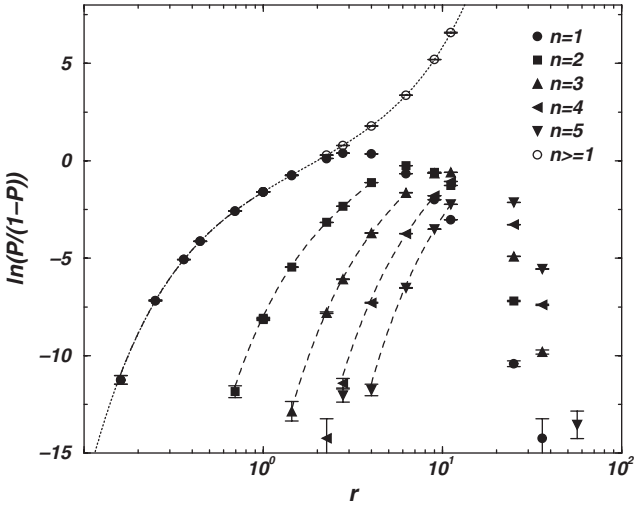

Fig. 4. The rescaled probability $\mathscr{P}^{(b)}_{N=30000^2}((1,0),n,r)$ in the form $\ln(\mathscr{P}/(1-\mathscr{P}))$ for different n. The dotted line shows the analytical result (1), while the dashed lines are fitted according to (17) using the parameters shown in Table I.

Just as for wrapping clusters on the cylinder, one might be tempted to find a systematic dependence of $C((1,0),n)$ and $\alpha((1,0),n)$ on n, such as an exponential and a second order polynomial, respectively. However, we were unable to identify these functions. Moreover, as the functional form (17) already differs from the corresponding function for wrapping clusters on the cylinder, it is not surprising that no similarities were found between their exponents and amplitudes.

2.5. Möbius Strip

The probability to obtain n windings on a Möbius strip is denoted in the following by $\mathscr{P}(\infty,n,r)$, where n encodes the number of winding

Table I. Multiple Winding Clusters (1, 0). The Numerical Results $\mathscr{P}_{N=30000^2}((1,0),n,r)$ Are Fitted within the Range Indicated Against (17)

n	r range	$C^{(s)}((1,0),n)$	$\alpha((1,0),n)$	$C^{(b)}((1,0),n)$	$\alpha((1,0),n)$
1	12/75 ··· 30/30	0.811(3)	1.568(3)	0.810(3)	1.566(3)
2	25/36 ··· 60/15	0.856(3)	7.771(12)	0.868(4)	7.813(14)
3	36/25 ··· 75/12	1.364(10)	19.02(4)	1.368(11)	19.02(5)
4	50/18 ··· 90/10	2.05(2)	33.91(8)	2.10(2)	34.05(10)
5	60/15 ··· 100/9	3.76(6)	53.94(16)	3.71(7)	53.82(19)

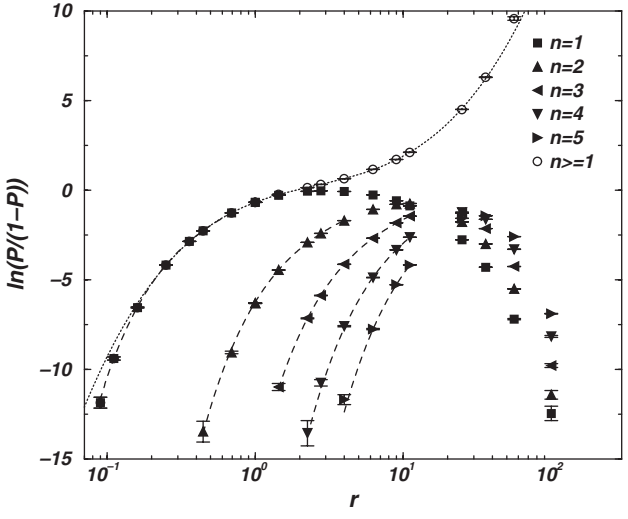

Fig. 5. The rescaled probability $\mathscr{P}^{(b)}_{N=30000^2}(\infty, n, r)$ in the form $\ln(\mathscr{P}/(1-\mathscr{P}))$ for different n. The dashed lines show the fitting results according to (20) using the parameters shown in Table II. The dotted line approximates the rescaled probability for r around 1 according to (21b).

clusters and their winding numbers as discussed above. Again, two different aspects can be investigated: the probability $\mathscr{P}(\infty, \geqslant 1, r)$ and the probability $\mathscr{P}(\infty, a, r)$ for each individual $a = 1, 2, \ldots$.

Figure 5 shows the numerical results for bond percolation and $N = 30000^2$, again in the reduced form $\ln(\mathscr{P}/(1-\mathscr{P}))$. The behavior is qualitatively similar to the one shown for multiple wrapping clusters on the torus, Fig. 4. Using the same ansatz as for wrapping clusters on the cylinder,[20]

$$\hat{\mathscr{P}}(\infty, n, r) \approx C(\infty, n)\, e^{-\alpha(\infty, n)/r}, \tag{20}$$

Table II. Winding Clusters on the Möbius Strip; Winding n Means $n/2$ Winding Clusters with Winding Number 2, if n Is Even, and $(n-1)/2$ Clusters with Winding Number 2 Plus a Single Cluster with Winding Number 1, if n Is Odd. The Numerical Results $\mathscr{P}_{N=30000^2}(\infty, n, r)$ Are Fitted within the Range Indicated Against (20)

n	r range	$C^{(s)}(\infty, n)$	$\alpha(\infty, n)$	$C^{(b)}(\infty, n)$	$\alpha(\infty, n)$
1	$9/100 \cdots 25/36$	0.982(3)	1.0401(14)	0.985(3)	1.0433(17)
2	$25/36 \cdots 60/15$	0.671(2)	5.832(9)	0.676(3)	5.849(11)
3	$36/25 \cdots 100/9$	0.780(2)	15.62(2)	0.774(3)	15.54(3)
4	$45/20 \cdots 100/9$	1.081(11)	30.93(10)	1.099(13)	31.08(12)
5	$60/15 \cdots 100/9$	1.44(6)	50.6(4)	1.51(6)	51.1(4)

the results shown in Table II have been derived. The same precautions as in Section 2.2 apply to the ranges shown in the table. While $\alpha(\infty, 1)$ can be conjectured to be $\pi/3$ with some confidence, the functional dependence of the exponents and amplitudes on n could not be found. Nevertheless, according to Fig. 5 the form (20) seems to work quite well.

In the spirit of ref. 10 we have tried to fit $\mathscr{P}_{N=30000^2}(\infty, \geqslant 1, r)$ against a third order polynomial in $\ln(r)$. The result

$$\ln\left(\frac{\mathscr{P}^{(s)}_{N=30000^2}(\infty, \geqslant 1, r)}{1-\mathscr{P}^{(s)}_{N=30000^2}(\infty, \geqslant 1, r)}\right) \approx -0.6798(7)+1.3525(9)\ln(r)-0.5648(9)\ln(r)^2+0.2021(3)\ln(r)^3 \tag{21a}$$

$$\ln\left(\frac{\mathscr{P}^{(b)}_{N=30000^2}(\infty, \geqslant 1, r)}{1-\mathscr{P}^{(b)}_{N=30000^2}(\infty, \geqslant 1, r)}\right) \approx -0.6793(8)+1.3545(10)\ln(r)-0.5689(11)\ln(r)^2+0.2033(4)\ln(r)^3 \tag{21b}$$

is shown for bond percolation in Fig. 5 as well. Similar to the results above, the main source of error is not statistical, but systematic, namely in the choice of the specific function. Nevertheless, the numerical result (21) will possibly serve as a reference for analytical findings.

3. CONCLUSION

Based on a large scale numerical simulation, this paper provides one of the first numerical confirmations of Pinson's analytical results for winding clusters on the torus, which are based on conformal field theory. It therefore also supports conformal invariance at the critical point.

By rewriting Pinson's results, it was possible to derive some asymptotes that have hitherto only been derived for the flat topology.[22, 23] These asymptotes have been used in the investigation of the probability of multiple, simultaneously wrapping clusters.

A similar numerical analysis has been carried out for the Möbius strip, which still awaits analytical treatment.

ACKNOWLEDGMENTS

The authors wish to thank Andy Thomas for his fantastic technical support. Without his help and dedication, this project would not have been possible. The authors also thank Dan Moore, Brendan Maguire, and Phil

Mayers for their continuous support. N.R.M. is very grateful to the Beit Fellowship, and to the Zamkow family. G.P. gratefully acknowledges the support of the EPSRC.

REFERENCES

1. M. Aizenman, On the number of incipient spanning clusters, *Nucl. Phys. B* **485**:551–582 (1997).
2. K. Binder and D. Stauffer, Monte Carlo studies of "random" systems, in *Applications of the Monte Carlo Method in Statistical Physics,* 2nd ed., K. Binder, ed., Topics in Current Physics, Vol. 36 (Springer-Verlag, Berlin/Heidelberg/New York, 1987), pp. 241–275.
3. J. Cardy, Critical percolation in finite geometries, *J. Phys. A: Math. Gen.* **25**:L201–L206 (1992), preprint hep-th/9111026.
4. J. Cardy, The number of incipient spanning clusters in two-dimensional percolation, *J. Phys. A: Math. Gen.* **31**:L105–L110 (1998).
5. P. di Francesco, H. Saleur, and J. B. Zuber, Relations between the coloumb gas picture and conformal invariance of two-dimensional critical models, *J. Stat. Phys.* **49**:57–79 (1987).
6. J. Hoshen and R. Kopelman, Percolation and cluster distribution. I. Cluster multiple labeling technique and critical concentration algorithm, *Phys. Rev. B* **14**:3438–3445 (1976).
7. C.-K. Hu and C.-Y. Lin, Universal scaling functions for numbers of percolating clusters on planar lattices, *Phys. Rev. Lett.* **77**:8–11 (1996).
8. K. Kaneda and Y. Okabe, Finite-size scaling for the Ising model and the Möbius strip and the Klein bottle, *Phys. Rev. Lett.* **86**:2134–2137 (2001).
9. H. Kesten, The critical probability of bond percolation on the square lattice equals 1/2, *Commun. Math. Phys.* **74**:41–59 (1980).
10. R. Langlands, C. Pichet, P. Pouliot, and Y. Saint-Aubin, On the universality of crossing probabilities in two-dimensional percolation, *J. Stat. Phys.* **67**:553–574 (1992).
11. W. T. Lu and F. Y. Wu, Ising model on nonorientable surfaces: Exact solution for the Möbius strip and the Klein bottle, *Phys. Rev. E* **63**:026107-1–026107-9 (2001).
12. W. Magnus, F. Oberhettinger, and R. P. Soni, *Formulas and Theorems for the Special Functions of Mathematical Physics* (Springer-Verlag, Berlin/Heidelberg/New York, 1966).
13. M. Matsumoto and T. Nishimura, Dynamic creation of pseudorandom number generators, in *Monte Carlo and Quasi-Monte Carlo Methods 1998* (Springer-Verlag, Berlin/Heidelberg/New York, 1998), preprint from http://www.math.h.kyoto-u.ac.jp/~matumoto/RAND/DC/dc.html.
14. B. Mendelson, *Introduction to Topology* (Allyn and Bacon, Inc., Boston/London/Sydney/Toronto, 1975).
15. N. R. Moloney and G. Pruessner, Asynchronously parallelized percolation on distributed machines, *Phys. Rev. E* **67**:037701-1–4 (2003), preprint cond-mat/0211240.
16. H. Nakanishi and H. E. Stanley, Scaling studies of percolation pheonmena in systems of dimensionality two to seven: Cluster numbers, *Phys. Rev. B* **22**:2466–2488 (1980).
17. M. E. J. Newman and R. M. Ziff, Efficient Monte Carlo algorithm and high-precision results for percolation, *Phys. Rev. Lett.* **85**:4104–4107 (2000).
18. M. E. J. Newman and R. M. Ziff, Fast Monte Carlo algorithm for site and bond percolation, *Phys. Rev. E* **64**:016706-1–16 (2001).
19. H. T. Pinson, Critical percolation on the torus, *J. Stat. Phys.* **75**:1167–1177 (1994).
20. G. Pruessner and N. R. Moloney, Numerical results for crossing, spanning and wrapping in two-dimensional percolation, *J. Phys. A: Math. Gen.* **36**:11213–11228 (2003).

21. D. C. Rapaport, Cluster number scaling in two-dimensional percolation, *J. Phys. A: Math. Gen.* **19**:219–304 (1986).
22. R. M. Ziff, On Cardy's formula for the critical crossing probability in 2d percolation, *J. Phys. A: Math. Gen.* **28**:1249–1255 (1995).
23. R. M. Ziff, Proof of crossing formula for 2d percolation, *J. Phys. A: Math. Gen.* **28**: 6479–6480 (1995).
24. R. M. Ziff, C. D. Lorenz, and P. Kleban, Shape-dependent universality in percolation, *Physica A* **266**:17–26 (1999).